



Palladium nanoparticle microemulsions: Formation and use in catalytic hydrogenation of *o*-chloronitrobenzene

Chunhua Liang^a, Jianguo Han^a, Kaihua Shen^{a,*}, Legang Wang^a,
Defeng Zhao^a, Harold S. Freeman^b

^a State Key Laboratory of Fine Chemicals, Dalian University of Technology, Dalian 116012, PR China

^b Department of Textile Engineering, Chemistry and Science, North Carolina State University, Raleigh, NC 27695-8301, USA

ARTICLE INFO

Article history:

Received 25 April 2010

Received in revised form 10 October 2010

Accepted 12 October 2010

Keywords:

Palladium nanoparticles
Microemulsion
Hydrogenation
o-Chloronitrobenzene

ABSTRACT

The formation and catalytic properties of well-dispersed palladium (Pd) nanoparticles in water-in-oil (w/o) microemulsions containing octadecyl amine polyoxyethylene ether (OAPE-5) and hydrogenated tallow amine (HTA) have been investigated. The size and structure of the nanoparticles were characterized by TEM and XRD analyses and the effects of microemulsion composition on particle sizes were assessed using FTIR spectroscopy. The results of TEM and XRD indicated that the particles were of a face centered cubic structure form and their mean diameter was 10 nm. Results of FTIR analysis indicated strong interactions between Pd nanoparticles and surfactant molecules. Use of these Pd nanoparticles for the hydrogenation of *o*-chloronitrobenzene in the presence of alkali produced a 3:1 ratio of aniline to *o*-chloroaniline and none of the frequently observed nitrobenzene or 2,2'-dichlorohydrozobenzene.

© 2010 Elsevier B.V. All rights reserved.

1. Introduction

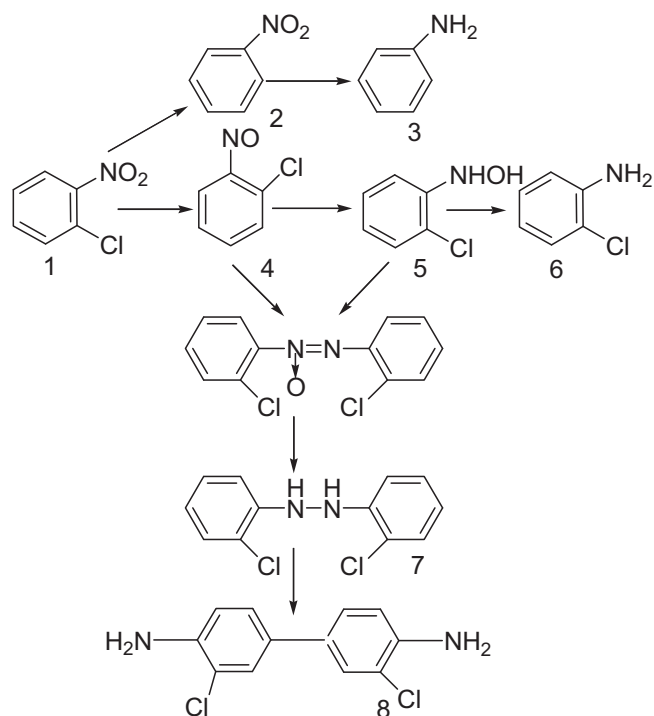
The electronic, optical, magnetic, and chemical properties of novel nanoparticles are known to be remarkably different from those of the corresponding bulk materials because of their extremely small sizes and high surface areas [1–3]. Many techniques have been used to prepare nanoparticles, including gas-evaporation [4,5], sputtering [6], co-precipitation [7], sol-gels [8], hydrothermal [9], and microemulsions [10–12]. Water-in-oil (w/o) microemulsions were transparent, isotropic liquid media with nanosized water droplets dispersed in a continuous oil phase and were stabilized by surfactant molecules at the water/oil interface. These surfactant-covered water pools offered a unique microenvironment for the formation of nanoparticles.

Catalytic hydrogenation using metallic palladium particles is an important process in organic synthesis. Owing to its stability on activated carbon, the commercially available palladium (Pd/C) catalyst is traditionally used in the heterogeneous hydrogenation of nitro-compounds or olefins. Results of a recent study revealed that Pd nanoparticles can be stabilized and dispersed in a water-in-CO₂ microemulsion for catalytic hydrogenation of olefins and nitro compounds at very rapid reaction rates [13]. Efficient hydrogenation is most likely due to the fact that the Pd nanoparticles in microemulsion are uniformly dispersed and

mixed with reactants and is comparable to a homogeneous catalytic system. The homogenization of normally heterogeneous catalysis utilizing microemulsions as media would have important applications in catalytic processes carried out in organic solvents. Microemulsions containing Pd nanoparticles have been used in the hydrogenation of styrene in iso-octane [14] and various olefins in organic solvents [15]. In those studies, microemulsions were found to be stable for about 15–20 min and the nanoparticles would then undergo aggregation. To prevent agglomeration of nanoparticles, many methods were considered [16–19]. A particularly interesting approach involved the use of an alkyl amine as both a stabilizer and co-surfactant in w/o microemulsions of nanoparticles. Use of fatty alkyl amines such as laurylamine [20], dodecylamine [21] and hexadecylamine [22] as stabilizers led to capping of nanoparticles by amine molecules and well-dispersed systems. Surfactants used in the formation of microemulsion systems have largely involved Aerosol OT (sodium bis(2-ethylhexyl) sulfosuccinate, a double-tailed anionic amphiphile) or CTAB (cetyl trimethylammonium bromide) as the choice of surfactant [15,23,24].

The *o*-chloronitrobenzene (1) hydrogenation reaction can be rather complex, with the variety of possible products illustrated in Scheme 1. The conversion of compound (1) to 2,2'-dichlorohydrozobenzene (7) is a key step in the Pd/C catalyzed synthesis of 3,3'-dichlorobenzidine (8), an important intermediate in diarylide yellow pigment production. In order to get high yield of 2,2'-dichlorohydrozobenzene (7), alkali is needed. Using high alkali levels and toluene as co-solvent, *o*-nitroschlorobenzene (4)

* Corresponding author. Tel.: +86 411 38393639; fax: +86 411 38393900.
E-mail address: shen.kh@yahoo.com.cn (K. Shen).



Scheme 1. Range of potential products from the catalytic hydrogenation of *o*-chloronitrobenzene in Pd/C systems.

and 2-nitrochloro-*N*-hydroxyaniline (**5**) formed initially and 2, 2'-dichlorohydrazobenzene formation occurred [25].

In the current work, attention is given to microemulsions made from mixtures containing a nonionic surfactant octadecyl amine polyoxyethylene ether (**5**) (OAPE-5) and hydrogenated tallow amine (HTA), and the control of microemulsion stability and conductivity by optimizing the proportion of OAPE-5 and HTA. The resultant microemulsion was employed in the hydrogenation of *o*-chloronitrobenzene. As a starting point, Pd nanoparticles were formed in the microemulsion and the effects of components used on microemulsion stability were investigated. The nature of the hydrogenation of *o*-chloronitrobenzene using this nanoparticle Pd-based microemulsion is outlined.

2. Experimental

2.1. General

All chemicals used were of analytical grade except hydrogenated tallow amine (HTA) and all were used without further purification. X-ray diffraction (XRD) measurements were performed using a Rigaku D/max 2400 X-ray diffractometer with Cu K α radiation. Transmission electron microscopy (TEM) images were taken with a FEI Tecnai 20 transmission electron microscope using an accelerating voltage of 200 kV. Fourier transfer infrared (FTIR) spectra were recorded in KBr discs using an EQUINOX55 (Bruker, Germany) instrument. HPLC analysis of reaction products was conducted using an Agilent 1100 chromatographic system (Waldbronn, Germany) equipped with a diode-array detector operating at 254 nm. Samples were dissolved in the mobile phase (methanol/H₂O = 70/30, v/v) and 2.00 μ l of the sample was injected. Hypersil ODS stainless steel columns (250 mm \times 4.5 mm, particle size 5 μ m) were employed. Selected-area electron diffraction (SAED) analysis was conducted using JEOL 2000EX microscope with an accelerating voltage of 200 kV.

2.2. Preparation of microemulsion

The procedure employed followed a literature method [26]. Toluene (7 mL), octadecyl amine polyoxyethylene ether (0.42 g; OAPE-5) and *n*-butyl alcohol (0.33 g) were placed in a 50 mL round bottomed flask and stirred with a magnetic stirrer. Then aqueous H₂PdCl₄ (0.17 mL, 0.05 M) was added. After stirring 30 min, hydrogenated tallow amine (HTA, 0.213 g), NaOH (0.017 g), and triethylamine (TEA, 0.082 g) were added to give a W value of 11. Following an additional 30 min, an optically transparent light yellow microemulsion was obtained.

2.3. Catalytic reduction

o-Chloronitrobenzene (0.134 g) and the prepared microemulsion were added into a 50 mL autoclave stainless steel and the autoclave was pressed and vented three times with N₂ and H₂, respectively. After the temperature reached to 30–80 °C and the pressure reached to 0.1–0.8 MPa, Pd²⁺ was reduced to metallic Pd by the hydrogen gas according to a previous study [27]. The hydrogenation reaction was performed with vigorous stirring under the setting hydrogen pressure (0.1–0.8 MPa) and the reaction terminated until the hydrogen pressure did not decline.

3. Results and discussion

3.1. Characterization of Pd nanoparticles

TEM and selected-area electron diffraction (SAED) analysis showed that Pd⁰ particles formed during the reduction process and that the microemulsion based on a mixture of OAPE-5 and HTA exhibited better stability than the one based on OAPE-5 alone (Figs. 1 and 2). Pd⁰ particles possessed a narrow size distribution (~10 nm), and SAED analysis showed that they were predominantly crystalline in nature with an fcc (face-centered cubic) structure. From Fig. 1, it can be seen that the Pd nanoparticles appeared to aggregate in the OAPE-5/*n*-butyl alcohol/toluene/H₂PdCl₄ microemulsion. It is likely that weak adsorption of OAPE-5 on Pd nanoparticles contributes to aggregation of particles during the subsequent reduction process.

Pd nanoparticles formed in our microemulsions were characterized by X-ray diffraction, and the results are shown in Fig. 3. The diffraction peaks at (1 1 1), (2 0 0) and (2 2 0) correspond to $2\theta = 39.98, 46.58, 67.91$, respectively, are indicative of a face-centered cubic (fcc) structure and are the same as observed following SAED analysis. It is interesting to note that the crystalline nature of Pd nanoparticles formed in our microemulsions were very similar to their face centered cubic crystal characteristics.

Fig. 4 provides a comparison of FTIR spectra of Pd nanoparticles formed in the OAPE-5/HTA combination (a) and in OAPE-5 alone (b), of pure HTA (c) and of pure OAPE-5 (d). No changes were found for the peak position of asymmetric and symmetric C–H stretching vibrations (3000–2800 cm⁻¹). The CH₂ peak at 1462 cm⁻¹ is typical of an all-trans methylene chain (1467 cm⁻¹). These results suggest that the alkyl chains are packed in a solid-like arrangement. However, a reduction in intensity of $\nu(\text{OH})$ (3390 cm⁻¹) in OAPE-5 confirms partial conversion of the –CH₂OH group to an aldehyde group [28]. The FTIR spectrum recorded in OAPE-5/HTA (a) reflected appreciable differences in the characteristic peaks of HTA (3253 cm⁻¹ ν_{as} N–H, 3166 cm⁻¹ ν_{s} N–H, 1603 cm⁻¹ δ N–H), due to coordination with Pd. While the characteristic peaks of OAPE-5 (ν OH 3395 cm⁻¹, ν C–O–C 1244 cm⁻¹, 1069 cm⁻¹, ν C–N 1298 cm⁻¹, 1124 cm⁻¹) were observed, they underwent shifts to slightly lower wave numbers, once the surfactant molecules were adsorbed on the nanoparticle surface, as indicated in Fig. 4a and b

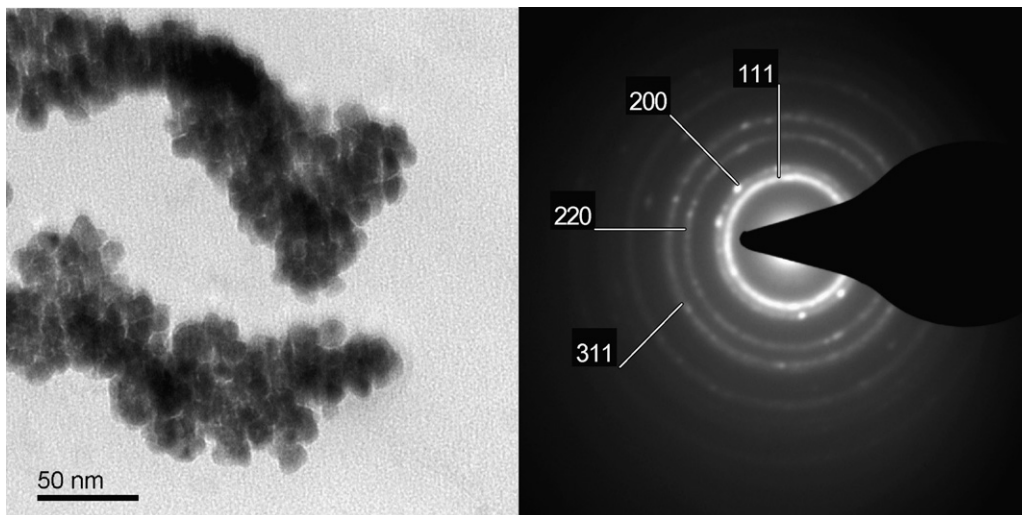


Fig. 1. TEM micrographs and electron diffraction of Pd nanoparticles collected from the OAPE-5/*n*-butyl alcohol/toluene/H₂PdCl₄ microemulsion after hydrogenation.

spectra (ν OH 3390 cm⁻¹, ν C–O–C 1238 cm⁻¹, 1069 cm⁻¹, ν C–N 1293 cm⁻¹, 1118 cm⁻¹). These results indicate that interactions exist not only between HTA and Pd but also between OAPE-5 and Pd, with the latter relatively weaker than the former.

Studies pertaining to the formation of Pd nanoparticles in OAPE-5 media were also undertaken. It was found the nature of the co-surfactant affected microemulsion stability and, consequently, the catalytic efficiency of the resultant Pd nanoparticles. *N,N'*-dimethyloctadecylamine did not form a stable water-in-oil microemulsion in the presence or absence of OAPE-5 or a solution of Na₂PdCl₄. Instead, aggregation readily occurred in the form of suspended black Pd particles. When *N*-octadecyl propylenediamine acetate was used as a co-surfactant, the microemulsion obtained had better stability than with other co-surfactants. Unfortunately, hydrogenation of *o*-chloronitrobenzene in the *N*-octadecyl propylenediamine acetate/OAPE-5 microemulsions did not occur because strong coordination between *N*-octadecyl propylenediamine acetate and Pd²⁺ prevented Pd nanoparticle formation.

3.2. Hydrogenation of *o*-chloronitrobenzene over Pd nanoparticles in the microemulsion

In the present study, the hydrogenation of *o*-nitrochlorobenzene in microemulsion systems was investigated, with conversion levels

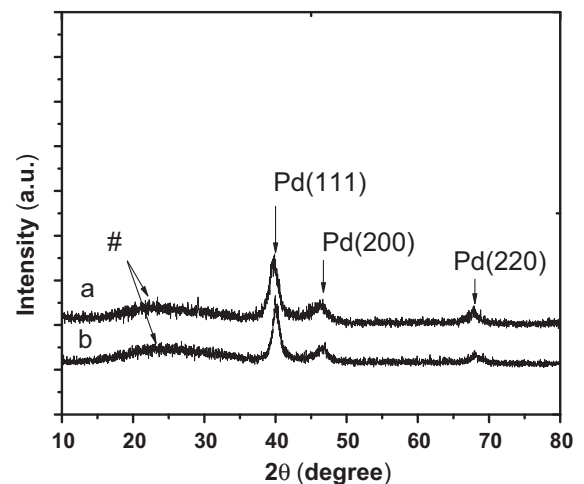


Fig. 3. X-ray diffractograms of Pd nanoparticles after hydrogenation in (a) OAPE-5/*n*-butyl/alcohol/toluene/H₂PdCl₄; (b) OAPE-5/HTA/*n*-butyl alcohol/toluene/H₂PdCl₄; #: Diffraction peaks from glass.

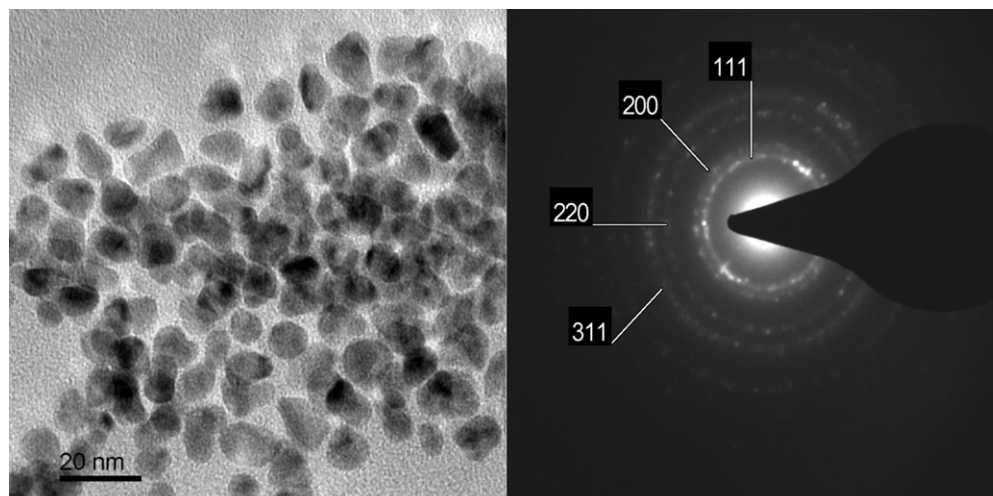


Fig. 2. TEM micrographs and electron diffraction of Pd nanoparticles collected from the OAPE-5/HTA/*n*-butyl alcohol/toluene/H₂PdCl₄ microemulsion after hydrogenation.

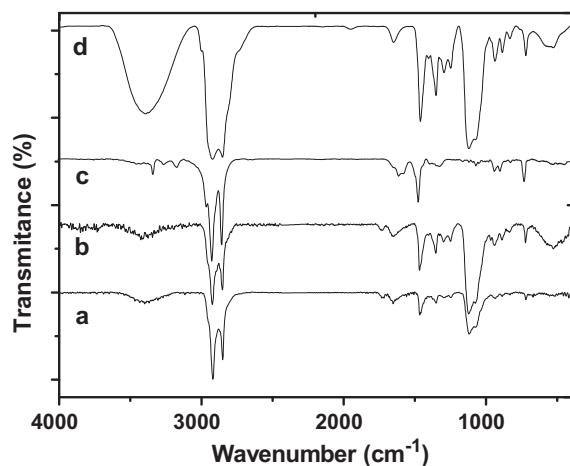


Fig. 4. FTIR spectra of Pd nanoparticles from microemulsions containing (a) OAPE-5/HTA protected Pd; (b) OAPE-5 capped with Pd; (c) pure HTA; (d) pure OAPE-5.

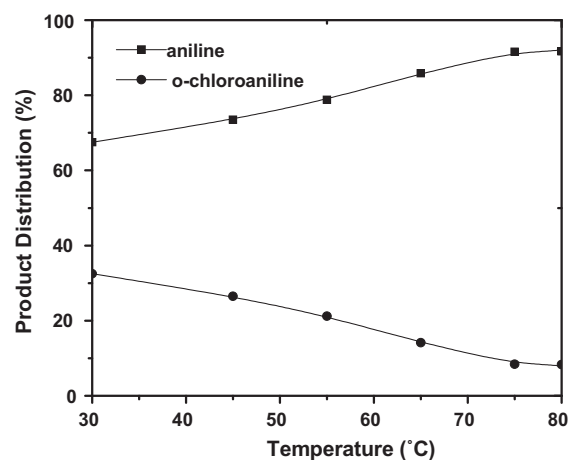


Fig. 5. Effect of temperature on proportion of aniline and *o*-chloroaniline formation in OAPE-5/HTA/NaOH/*n*-butyl alcohol/toluene/H₂PdCl₄ (1:1:0.5:0.5:0.01) microemulsion at 0.6 MPa.

and selectivity assessed using HPLC analysis. Table 1 shows results from hydrogenation of *o*-chloronitrobenzene in two microemulsion systems. In the OAPE-5 system, conversion and selectivity were poor. In addition, hydrogenation was incomplete in the absence of HTA co-surfactant but the addition of HTA and alkali dramatically enhanced the reaction speed. In the typical hydrogenation of *o*-chloronitrobenzene on Pd, dechlorination occurs during reduction and aniline becomes the main product instead of 2,2'-dichlorohydrazobenzene. In the OAPE-based microemulsion system, HTA functioned not only as a stabilizer of nanoparticles but also as an agent for dechlorination, and aniline formation was predominant if either NaOH or TEA was present.

Table 1

Product distribution of hydrogenation of *o*-chloronitrobenzene in a Pd nanoparticle based microemulsion^a.

Alkaline agent	Aniline	<i>o</i> -Chloroaniline	Nitrobenzene	Conversion (%)	Reaction time (min)
OAPE-5	36.48	3.42	44.19	84.09	<22
OAPE-5/NaOH	67.01	26.36	6.63	100	<18
OAPE-5/TEA	57.82	4.51	29.20	91.53	<23
OAPE-5/HTA	75.35	24.65	0	100	<10
OAPE-5/(NaOH:HTA) ^b	78.8	21.2	0	100	<16
OAPE-5/(TEA:HTA) ^c	78.05	21.95	0	100	<12

^a *o*-Chloronitrobenzene/OAPE-5/alkali/H₂PdCl₄ (1:1:1:0.01), *o*-chloronitrobenzene, 55 °C, 0.6 MPa.

^b NaOH:HTA = 1:1.

^c TEA:HTA = 1:1.

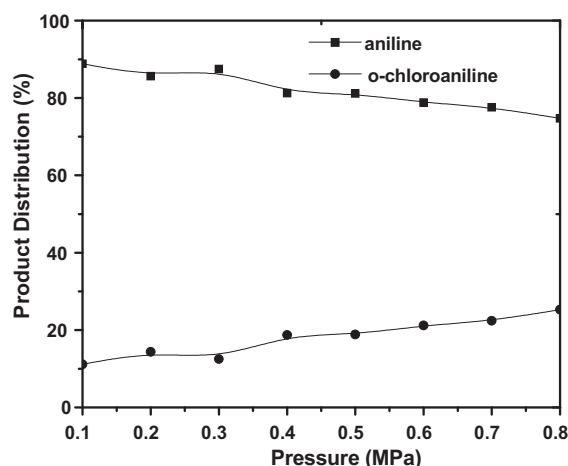


Fig. 6. Effect of pressure on proportion of aniline and *o*-chloroaniline formation in OAPE-5/HTA/NaOH/*n*-butyl alcohol/toluene/H₂PdCl₄ (1:1:0.5:0.5:0.01) microemulsion at 55 °C.

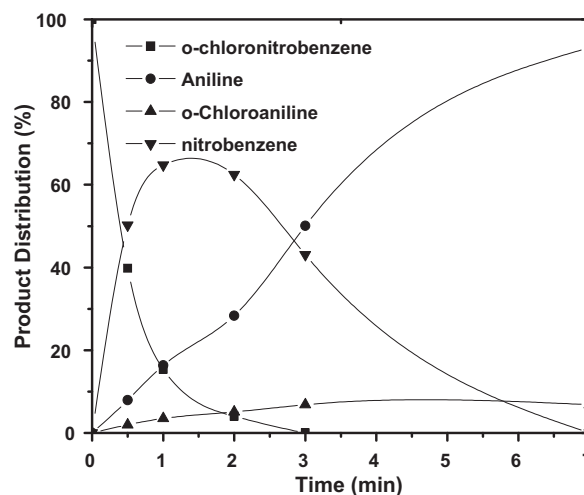


Fig. 7. The relative changes in *o*-nitrochlorobenzene, nitrobenzene, aniline and *o*-chloroaniline levels during hydrogenation in a Pd nanoparticle based microemulsion at 80 °C and 0.3 MPa.

The effects of temperature and pressure on the hydrogenation of *o*-chloronitrobenzene were investigated (cf. Figs. 5 and 6). While, the amount of aniline increased as the temperature increased, aniline levels decreased with increased pressure.

It is known that high surfactant levels can enhance mass transfer rates during hydrogenation [29]. In the present microemulsion system, intermediate compounds (4) and (5) were easily reduced to aniline or *o*-chloroaniline. It is illustrated Fig. 7 that high levels of nitrobenzene were detected at early stages of the reaction, and the rate of dechlorination was higher than nitro group reduction. It has

been reported that the adsorption of *o*-chloroaniline on Pd catalysts is inferior to the adsorption of *o*-chloronitrobenzene, retarding the conversion of *o*-chloroaniline to aniline [30], which is in agreement with our results. At the end of the present hydrogenation, aniline and *o*-chloroaniline were obtained, and the proportion of aniline was up to 93%.

4. Conclusions

The preparation of Pd nanoparticles in a nonionic microemulsion consisting of OAPE-5/HTA/*n*-butyl alcohol/toluene/H₂PdCl₄ can be achieved by the reduction of H₂PdCl₄ with H₂ at 55 °C and confirmed using SAED and X-ray diffraction analyses. It is also clear that the main factor in the preparation of stable Pd nanoparticles in the OAPE-5/HTA system is the ratio of co-surfactant HTA to OAPE-5. Similarly, adding a controlled amount of octadecylamine or alkyl-dimethyl tertiary amines helps stabilize Pd nanoparticles; however, the latter additives give Pd nanoparticles that are stable for about 30–50 min then gradually lose their catalytic properties due to aggregation.

Results of this study also indicate that the hydrogenation of *o*-chloronitrobenzene in this Pd-containing microemulsion gives good yields of aniline, via nitro group reduction and dechlorination, but none of the corresponding hydrazobenzene even in the presence of alkali.

Acknowledgement

Project supported by the National Natural Science Foundation of China (Grant No. 20976025).

References

- [1] G.A. Ozin, Nanochemistry: synthesis in diminishing dimensions, *Adv. Mater.* 4 (1992) 612–649.
- [2] R.W. Cahn, Nanostructures come of age, *Nature* 359 (1992) 591–592.
- [3] A. Henglein, Small-particle research: physicochemical properties of extremely small colloidal metal and semiconductor particles, *Chem. Rev.* 89 (1989) 1861–1873.
- [4] M.T. Swihart, Vapor-phase synthesis of nanoparticles, *Curr. Opin. Colloid Interface Sci.* 8 (2003) 127–133.
- [5] R. Uyeda, The morphology of fine metal crystallites, *J. Cryst. Growth* 24–25 (1974) 69–75.
- [6] P. Fayet, L. Woste, Experiments on size-selected metal cluster ions in a triple quadrupole arrangement, *Z. Phys. D: Atoms Mol. Clust.* 3 (1986) 177–182.
- [7] Z.X. Tang, C.M. Sorensen, K.J. Klabunde, G.C. Hadji-panayis, Preparation of manganese ferrite fine particles from aqueous solution, *J. Colloid Interface Sci.* 146 (1991) 38–52.
- [8] A. Kaiser, A. Goersmann, U. Schubert, Influence of the metal complexation on size and composition of Cu/Ni nano-particles prepared by sol-gel processing, *J. Sol-Gel Sci. Technol.* 8 (1997) 795–799.
- [9] S. Komarneni, R. Roy, E. Breval, M. Ollinen, Y. Suwa, Hydrothermal route to ultrafine powders utilizing single and diphasic gels, *Adv. Ceram. Mater.* 1 (1986) 87–92.
- [10] K. Osseo-Asare, F.J. Arriagada, Synthesis of nanosize particles in reverse microemulsions, *Ceram. Trans.* 12 (1990) 3–16.
- [11] M.P. Pileni, Reverse micelles as microreactors, *J. Phys. Chem.* 97 (1993) 6961–6973.
- [12] V. Pillai, P. Kumar, M.J. Hou, P. Ayyub, D.O. Shah, Preparation of nanoparticles of silver halides, superconductors and magnetic materials using water-in-oil microemulsions as nano-reactors, *Adv. Colloid Interface Sci.* 55 (1995) 241–269.
- [13] H. Ohde, C.M. Wai, H. Kim, J. Kim, M. Ohde, Hydrogenation of olefins in supercritical CO₂ catalyzed by palladium nanoparticles in a water-in-CO₂ microemulsion, *J. Am. Chem. Soc.* 124 (2002) 4540–4541.
- [14] H. Sato, T. Ohtsu, I. Komasa, Preparation of ultrafine palladium particles in reverse micelles and application for hydrogenation catalysts, *J. Chem. Eng. Jpn.* 35 (2002) 255–262.
- [15] B. Yoon, H. Kim, C.M. Wai, Dispersing palladium nanoparticles using a water-in-oil microemulsion-homogenization of heterogeneous catalysis, *Chem. Commun.* 9 (2003) 1040–1041.
- [16] K.R. Gopidas, J.K. Whitesell, M.A. Fox, Synthesis, characterization, and catalytic applications of a palladium-nanoparticle-cored dendrimer, *Nano Lett.* 3 (2003) 1757–1960.
- [17] A. Denicourt-Nowicki, M. Romagné, A. Roucoux, N-(2-Hydroxyethyl)ammonium derivatives as protective agents for Pd (0) nanocolloids and catalytic investigation in Suzuki reactions in aqueous media, *Catal. Commun.* 10 (2008) 68–70.
- [18] M.C. Daniel, D. Astruc, Gold nanoparticles: assembly, supramolecular chemistry, quantum-size-related properties, and applications toward biology, catalysis, and nanotechnology, *Chem. Rev.* 104 (2004) 293–346.
- [19] D.K. Mukherjee, Potential application of palladium nanoparticles as selective recyclable hydrogenation catalysts, *J. Nanopart. Res.* 10 (2008) 429–436.
- [20] C.R.K. Rao, V. Lakshminarayanan, D.C. Trivedi, Synthesis and characterization of lower size, laurylamine protected palladium nanoparticles, *Mater. Lett.* 60 (2006) 3165–3169.
- [21] M. Aslam, E.A. Schultz, T. Sun, T. Meade, V.P. Dravid, Synthesis of amine-stabilized aqueous colloidal iron oxide nanoparticles, *Cryst. Growth Des.* 7 (2007) 471–475.
- [22] N. Cordente, M. Respaud, F. Senocq, M.J. Casanove, C. Amiens, B. Chaudret, Synthesis and magnetic properties of nickel nanorods, *Nano Lett.* 1 (2001) 565–568.
- [23] D. Das, P.K. Das, Improving the lipase activity profile in cationic water-in-oil microemulsions of hydroxylated surfactant, *Langmuir* 19 (2003) 9114–9119.
- [24] Y. He, B. Yang, G. Cheng, Controlled synthesis of CeO₂ nanoparticles from the coupling route of homogeneous precipitation with microemulsion, *Mater. Lett.* 57 (2003) 1880–1884.
- [25] K. Shen, S. Li, D.H. Choi, Catalytic hydrogenation of *o*-nitrochlorobenzene to 3, 3'-dichlorobenzidine, *Bull. Korean. Chem. Soc.* 23 (2002) 1785–1789.
- [26] S. Eriksson, U. Nylén, S. Rojas, M. Boutonnet, Preparation of catalysts from microemulsions and their applications in heterogeneous catalysis, *Appl. Catal. A: Gen.* 265 (2004) 207–219.
- [27] M. Boutonnet, J. Kizling, P. Stenius, G. Maire, The preparation of monodisperse colloidal metal particles from microemulsions, *Colloids Surf.* 5 (1982) 209–225.
- [28] S. Bertarione, D. Scarano, A. Zecchina, V. Johaneck, J. Hoffmann, S. Schauermaier, J. Libuda, G. Rupprechter, H.J. Freund, Surface reactivity of Pd nanoparticles supported on polycrystalline substrates as compared to thin film model catalysts: infrared study of CH₃OH adsorption, *J. Catal.* 233 (2004) 64–73.
- [29] A.S. Mayer, L. Zhong, G.A. Pope, Measurement of mass-transfer rates for surfactant-enhanced solubilization of nonaqueous phase liquids, *Environ. Sci. Technol.* 33 (1999) 2965–2972.
- [30] B. Coq, A. Tijani, F. Figuéras, Particle size effect on the kinetics of *p*-chloronitrobenzene hydrogenation over platinum/alumina catalysts, *J. Mol. Catal.* 68 (1991) 331–345.